Arc fusion splicing of hollow-core photonic bandgap fibers for gas-filled fiber cells

R. Thapa, K. Knabe, K. L. Corwin, and B. R. Washburn
Kansas State University, Dept. of Physics, 116 Cardwell Hall, Manhattan, KS 66506
washburn@phys.ksu.edu

Abstract: The difficulty of fusion splicing hollow-core photonic bandgap fiber (PBGF) to conventional step index single mode fiber (SMF) has severely limited the implementation of PBGFs. To make PBGFs more functional we have developed a method for splicing a hollow-core PBGF to a SMF using a commercial arc splicer. A repeatable, robust, low-loss splice between the PBGF and SMF is demonstrated. By filling one end of the PBGF spliced to SMF with acetylene gas and performing saturation spectroscopy, we determine that this splice is useful for a PBGF cell.

©2006 Optical Society of America

OCIS codes: (060.4510) Optical communications; (120.3930) Metrological Instrumentation; (300.1030) Absorption; (230.3990) Microstructure devices;

References and links

1. F. Benabid, P. S. Light, F. Couny, and P. S. J. Russell, "Electromagnetically-induced transparency grid in acetylene-filled hollow-core PCF," Opt. Express **13**, 5694-5703 (2005).
2. S. Ghosh, J. E. Sharping, D. G. Ouzounov, and A. L. Gaeta, "Resonant optical interactions with molecules confined in photonic band-gap fibers," Phys. Rev. Lett. **94**, 093902-1 (2005).
3. J. Henningsen, J. Hald, and J. C. Peterson, "Saturated absorption in acetylene and hydrogen cyanide in hollow-core photonic bandgap fibers," Opt. Express **13**, 10475-10482 (2005).
4. R. Thapa, K. Knabe, M. Faheem, A. Naweed, O. L. Weaver, and K. L. Corwin, "Saturated absorption spectroscopy of acetylene gas inside large-core photonic bandgap fiber," Opt. Lett. **31**, 2489-2491 (2006).
5. T. Ritari, J. Tuominen, H. Ludvigsen, J. C. Petersen, T. Sørensen, T. P. Hansen, and J. C. Simonsen, "Gas sensing using air-guiding photonic bandgap fibers," Opt. Express **12**, 4080-4087 (2004).
6. F. Benabid, F. Couny, J. C. Knight, T. A. Birks, and P. S. J. Russell, "Compact, stable and efficient all-fibre gas cells using hollow-core photonic crystal fibres," Nature **434**, 488-491 (2005).
7. T. Ritari, G. Genty, and H. Ludvigsen, "Supercontinuum and gas cell in a single microstructured fiber cell," Opt. Lett. **30**, 3380-3382 (2005).
8. A. Yablon, *Optical fiber fusion splicing* (Springer, Heidelberg, 2005).
9. P. S. Light, F. Couny, and F. Benabid, "Low optical insertion-loss and vacuum-pressure all-fiber acetylene cell based on hollow core PCF," Opt. Lett. **31**, 2538-2540 (2006).
10. P. J. Bennett, T. M. Monro, and D. J. Richardson, "Toward practical holey fiber technology: fabrication, splicing, modeling, and characterization," Opt. Lett. **24**, 1203-1205 (1999).
11. B. Bourliaguet, C. Paré, F. Émond, A. Croteau, A. Proulx, and R. Vallée, "Microstructured fiber splicing," Opt. Express **11**, 3412-3417 (2003)..
12. Crystal Fibre A/S, http://www.crystal-fibre.com/support/faq.shtm.
13. L. Xiao, W. Jin, M. S. Demokan, H. L. Ho, Y. L. Hoo, and C. Zhao, "Fabrication of selective injection microstructured optical fibers with a conventional fusion splicer," Opt. Express **13**, 9014-9022 (2005).
14. Corning SMF-28e optical fiber product information, http://www.corning.com/opticalfiber/.
15. Crystal Fibre A/S HC19-1550-01 product information, http://www.crystal-fibre.com.
16. Crystal Fibre A/S HC-1550-02 product information, http://www.crystal-fibre.com.
17. J. H. Chong and M. K. Rao, "Development of a system for laser splicing photonic crystal fiber," Opt. Express **11**, 1365-1370 (2003).
18. D. Gloge, "Weakly guiding fibers," Appl. Opt. **10**, 2252-8 (1971).
19. C. R. Pollack, *Fundamentals of Optoelectronics* (Irwin, Chicago, 1995), Chap. 11.
20. G.-i. Kweon and I.-S. Park, "Splicing losses between dissimilar optical waveguides," J. of Lightwave Technol. **17**, 690-703 (1999).

1. Introduction

Photonic bandgap fibers (PBGF) are optical waveguides that will serve as a key technology to enable future advances in frequency metrology, spectroscopy, and quantum optics. A PBGF is a low-loss waveguide whose hollow core can be filled with a fluid, allowing light to interact with the fluid while being guided by the PBGF geometry. Recently, much progress has been made using gas-filled PBGF, including the observation of resonant interactions and electromagnetically-induced transparency in acetylene-filled fibers, which has important applications toward all-optical fiber communications [1, 2]. Saturation spectroscopy, for higher-accuracy portable optical frequency references, has also been demonstrated [3, 4]. Even linear interactions are significantly enhanced in PBGFs, resulting in the development of gas sensors [5] and Doppler- and pressure-broadened frequency references [6, 7].

Splices between microstructured fibers and step index single-mode fibers (SMF) are difficult to create, because the air holes in the fiber tend to collapse at the high temperatures required to form a strong splice (see Ref. [8] and references therein). Splicing solid-core microstructured optical fibers to SMF is typically accomplished with filament splicers [6, 9, 10], but has also been demonstrated using an arc splicer [11]. Indeed, splicing SMF to hollow-core PBGF is even more difficult due to the presence of the large guiding hole, and this difficulty limits the use of these fibers in laboratory experiments or in commercial products. However, successful splices between hollow-core PBGF and SMF have been made using a filament-based fusion splicer, and are commercially available [12]. Furthermore, arc splicers have been used to systematically investigate the collapse of air holes in PBGF for selective injection [13], but until now, no low-loss, robust splices have been made with the relatively inexpensive and ubiquitous arc fusion splicer.

Many applications of PBGF require the fabrication of a PBGF cell, in which a length of PGBF is filled with a gas or liquid and spliced to solid-core single-mode fiber on each end. This cell is doubly difficult to produce since 1) two low-loss splices between the SMF and PBGF fiber must be made and 2) at least one splice must be made while keeping the gas in the PBGF microstructures. Such PBGF cells have been created [6, 7, 9] where the first splice between the PBGF and SMF is made in air, while the second splice to SMF must be made in a gas atmosphere. In fact, PBGF have been sealed after being filled by acetylene gas [6], but this technique relies on the use of an expensive, filament-based fusion splicer. Another clever method of making gas-filled PBGF cells involves splicing the PBGF to SMF in a helium and acetylene gas purge using a filament splicer [9]. The helium diffuses from the PBGF, leaving only high purity acetylene in the cell. Nevertheless, a simple recipe for splicing PBGF to SMF using a conventional arc fusion splicer has until now been lacking. Here we demonstrate a repeatable, robust, low-loss splice between a hollow-core PBGF and SMF. The performance of this fiber compares favorably with a commercially made spliced fiber.

2. Fusion splicing hollow-core PBGF to SMF

2.1 Specific fibers used in this study

Two types of hollow-core PBGF, both purchased from Crystal Fibre A/S, are discussed in this study. The PBGFs were spliced to Corning® SMF-28e® SMF using an Ericsson FSU-995 electric arc fusion splicer. The first PBGF, part number HC-1550-02, has a hole diameter of 10.9 µm and a mode overlap of >90 % with the SMF. The second PBGF, part number HC19-1550-01, has a hole diameter of 20 µm. The significant fiber parameters are listed in Table 1.

Table 1. Fiber Parameters for the PBGF and the Single-Mode Fiber

Fiber Name	Core diameter	Mode-field diameter	Numerical Aperture	Hole Separation Λ
HC-1550-02	10.9 µm	7.5 µm[†]	0.12[†]	3.8
HC19-1550-01	20 µm	13 µm[‡]	0.13[‡]	3.9
SMF-28e	8.2 µm	10.4 µm[†]	0.14	--

[†]Values given at 1550 nm [14]. [‡]Values given at 1570 nm [15, 16].

2.2 Splicing procedure using an electric arc splicer

Filament splicers are generally preferred for fusion splicing PBGFs since they heat the fiber more slowly and uniformly. Our goal, which is motivated largely by the cost and popularity of arc fusion splicers, is to mimic this performance with a more common electric arc fusion splicer. One difficulty in splicing hollow-core PBGF is avoiding the collapse of the microstructures, because temperatures that are high enough to form a strong splice also allow the glass to flow. Splicing PBGF is particularly difficult using an electric arc splicer because the fibers are heated very rapidly during the arc. Thus, we have developed a multi-step splice procedure involving a short, high current arc followed by a long, low current arc. In general, the amount of current used in this process is less than that of a conventional splicing procedure.

The geometry of the fusion splicer is illustrated in Fig. 1. There are two parameters that define the distance of the fibers from the electric arc and from each other. The first parameter called "gap" measures the distance between the two fibers. Zero gap, which occurs at a position called the "touch point" indicates that the fibers are butt-coupled. Negative gaps, here called "overlap", indicate that the fibers are pushed further together than they were when butt-coupled. The second parameter called "offset" indicates the displacement of the touch point from the electrode axis. In all splices, the fibers are prepared by mechanically stripping the coating away from the last ~2.5 cm of fiber, and cleaved using a Fujikura CT-04B cleaver.
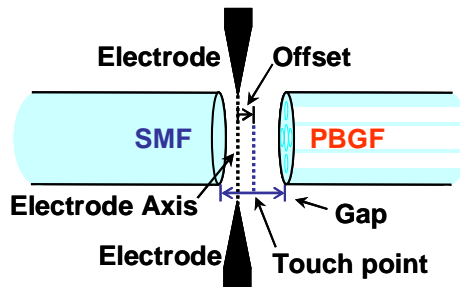

Fig. 1. The fusion splicer geometry. Two variable parameters, gap/overlap and offset, determine the position of the fibers with respect to the electrode axis.

The optimum procedure for splicing PBGF to SMF was developed by attempting more than twenty splices with a wide range of splice parameters. The resulting optimized program for splicing SMF-28e® to the 10.9 μm PBGF HC-1550-02 is as follows. The splicing program first aligns the fibers and produces a short burst of current (pre-fuse) to remove any contamination present in the fiber end. This pre-fuse also removes any moisture in the microstructures that will cause the splice to be fragile. Next, the fibers are briefly butt-coupled at the touch point, and a gap of +10 μm is made. The offset is set to 260, placing the electrodes roughly 5 μm closer to the SMF than the PBGF (as determined using Ref. [13]). The butt-coupled loss from the SMF to the 10.9 μm PBGF is typically 1.0 dB. The nonzero offset is a critical parameter in the splicing since it ensures that the SMF is heated more strongly than the PBGF, to prevent the collapse of the air holes [17]. Fusion current 1 is set to 10 mA and applied for 0.2 s, which softens both fiber ends and prepares the fibers to be overlapped and fused together upon physical contact in the next process. Care must be taken while choosing this current level because a low arc current leads to a mechanical deformation during the overlapping stage, while a high current causes a change in the glass geometry resulting in a poor quality splice. If fusion current 1 is reduced from the optimum splicing condition of 10 mA to 9 mA for the same duration (0.2 s), the resulting splice loss is approximately the same in both cases, but the mechanical strength of the splice is greatly reduced. If for a constant fusion current 1 (10 mA) the time is increased beyond 0.2 s, the PBGF end deforms or collapses completely under surface tension, forming a spherical end.

Fusion current 2 starts when the fiber ends actually touch and press together in order to overlap and to fuse. During this phase, the current is reduced to 7 mA for 12 s while the fibers are pushed together to a negative gap, or overlap, of 10 µm. Increasing the overlap at optimum arc current to 15 µm gives a better mechanical strength (the splice breaking when bent at a radius of 1.5 cm compared to 1.7 cm) with comparable or slightly higher splice loss, while a smaller overlap of 5 µm gives a splice with comparable loss but which is extremely fragile. To complete the procedure the fusion current 3 is set to 6.5 mA for 3 s, while the splice anneals. Figure 2 illustrates the loss with respect to the butt-coupled transmission measured during the splicing procedure.

The splice routine was altered for splicing the SMF-28e® to the 20 µm PBGF HC19-1550-01. The only significant change in the program was the increase in the overlap from 10 µm to 15 µm in order to compensate for the larger hole diameter.

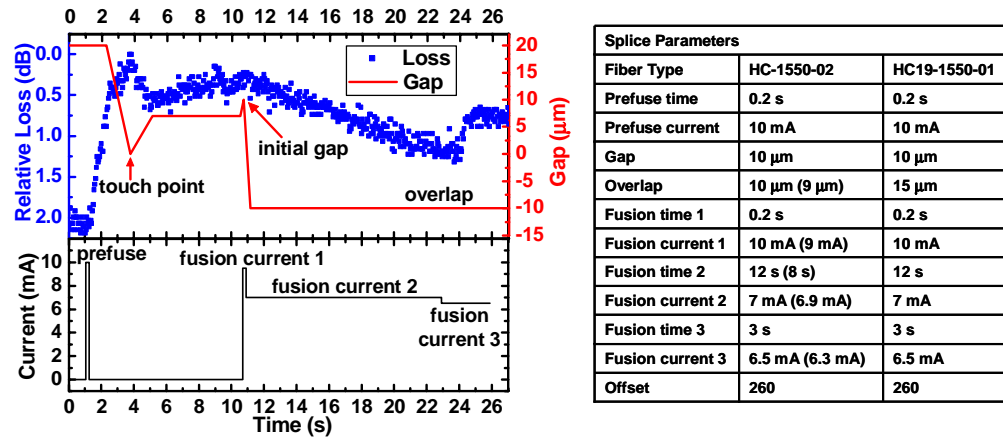| Splice Parameters		
Fiber Type	HC-1550-02	HC19-1550-01
Prefuse time	0.2 s	0.2 s
Prefuse current	10 mA	10 mA
Gap	10 µm	10 µm
Overlap	10 µm (9 µm)	15 µm
Fusion time 1	0.2 s	0.2 s
Fusion current 1	10 mA (9 mA)	10 mA
Fusion time 2	12 s (8 s)	12 s
Fusion current 2	7 mA (6.9 mA)	7 mA
Fusion time 3	3 s	3 s
Fusion current 3	6.5 mA (6.3 mA)	6.5 mA
Offset	260	260

Fig. 2. The relative loss with respect to the butt-coupled transmission from the SMF to the 10.9 µm PBGF during the fusion procedure. The gap curve is estimated from the splice parameters, the Ericsson FSU-995-FA fusion splicer manual, and the relative loss curve. The values in parenthesis indicate altered parameters for new electrodes.

2.3 Splice loss between SMF and PBGF

The splice loss is determined directly by measuring the transmission of a 1534 nm laser source through the splice, in both directions, using the following procedure. To measure the loss from SMF to PBGF, first the cw laser light is injected into the SMF fiber and the output power is measured. Then the SMF is spliced to the PBGF and the output power from the PBGF is measured. To measure the splice loss from the PBGF to SMF, the other end of the PBGF is subsequently spliced to another SMF and the output power is again measured.

The measured loss for splices of SMF to both the 20 µm and the 10.9 µm PBGFs are listed in Table 2. For both splices, the most unique feature is the non-reciprocity of the splice loss: the splice loss as measured from the SMF to PBGF is different from that measured in the opposite direction from the PBGF to SMF. In the 20 µm HC19-1550-01 fiber, splice loss from SMF to PBGF varies from 0.3 dB to 0.5 dB whereas splice loss from PBGF to SMF is more than 2 dB. The splice loss non-reciprocity is less prominent in 10.9 µm PBGF.

To verify the reproducibility of the procedure we made a series of splices measuring the loss in one direction. Four 20 µm SMF/PBGF splices were made on over the course of three weeks using the above recipe that had an average splice loss of 0.42 dB with a standard deviation of 0.09 dB. Also, five 10 µm SMF/PBGF splices were made with an average loss of 1.74 dB with a standard deviation of 0.19 dB. These results determine the range of values in Table 2. As further evidence for the splice reproducibility, a series of consecutive splices were made eight months after the development of the procedure. We had to replace the

splicer's electrodes since our initial reproducibility study above, but after a slight optimization the recipe worked well. The modified parameters for new electrodes are listed in Fig. 2. For the 10 μm fiber, we performed five SMF/PBGF splices in quick succession, taking about 20 minutes per splice, using the same splice parameters. Each splice was successful on the first attempt with the loss values of 1.8 dB, 1.5 dB, 1.8 dB, 1.9 dB, and 1.7 dB for the five splices.

Table 2. Measured Non-Reciprocal Splice Loss between PBGF to SMF

Splice Type	PBGF Core diameter	Loss from SMF to PBGF	Loss from PBGF to SMF
SMF-28e/HC-1550-02	10.9 μm	1.5-2.0 dB	2.6-3.0 dB
SMF-28e/HC19-1550-01	20 μm	0.3-0.5 dB	> 2.0 dB[†]

[†]Value was determined indirectly from the transmission through 20 μm PBGF cells.

Unfortunately the splice loss depends on the orientation of the PBGF, which we attribute to the multimode nature of the PBGF. To see this effect, fiber cells of both 10.9 and 20 μm fiber were made and the splices were fixed to a table. For example when one 20 μm PBGF cell was moved randomly, the loss varied erratically from 2.2 to 6.0 dB through the entire cell. For a 10.9 μm fiber cell a smaller change from 4.2 to 5.3 dB was observed.

A physical explanation of the observed splice loss is difficult due in part to the complicated mode structure of the PBGF. This measured splice loss can be explained rigorously by computing the overlap integral between the PBGF and SMF modes. Unfortunately the determination of this integral is impossible since the amount of energy in each guided mode is typically unknown [8]. Also, it is difficult to compute the number of modes of the PBGF without resorting to a numerical method for computing the modes.

Qualitative arguments based on the theory of step-index fibers [18] can be used to explain the observed loss and the non-reciprocal loss. An estimate of the minimum loss can be computed from the mode overlap of two Gaussian profiles with mode field radii r_1 and r_2. This overlap integral (assuming no axial mismatch) can be evaluated to give the minimum splice loss in dB as [19]

$$10 Log_{10} \left(4 r_1^2 r_2^2 \left(r_1^2 + r_2^2 \right)^{-2} \right). \tag{1}$$

Using this equation the minimum loss for the 10 μm PBGF to SMF splice is 0.45 dB while the minimum splice loss for the 20 μm PBGF to SMF splice is 0.21 dB. Interestingly, this approximation predicts that the 20 μm PBGF will have a lower minimum splice loss than the 10.9 μm PBGF, which is indeed observed.

The crude splice loss approximation given in Eq. (1) based on mode-field radii does not predict the non-reciprocal loss. However, this non-reciprocal loss can be explained in terms of mode mismatching between multimode waveguides [20]. The problem here is similar to the coupling between a SMF and a multimode fiber (MMF) at a given optical wavelength. For this scenario, there is a general rule that the loss from a small core fiber to a large core fiber be smaller than the loss in the other direction. In the case of coupling from SMF to MMF the loss is expected to be small [8]. The mode field radius of the SMF is smaller than that of the MMF so it can easily couple to the lowest order modes of the MMF. The opposite behavior occurs when coupling from the MMF to SMF. Here, higher order modes will be excited in the MMF that will not couple well to the SMF. From these arguments, it is expected that a larger asymmetry in splice loss will occur with a larger number of modes in the PBGF. Due to its larger diameter, the 20 μm PBGF supports more modes (~ 10 modes) than the 10.9 μm fiber (~ 1-3 modes). Thus the HC19-1550-01/SMF-28e splice should exhibit a more prominent non-reciprocal splice loss than the 10 μm PBGF. As described above, the 20 μm PBGF to SMF loss was much more susceptible to fiber positioning than the

10.9 μm PBGF to SMF loss. The observation is consistent with the 20 μm PBGF containing more modes than the 10.9 μm PBGF.

Figure 3 shows a micrograph of the HC-1550-02/SMF-28e splice. In general the splices are mechanically strong and can be bent to a ~1.5 cm circular radius before breaking.
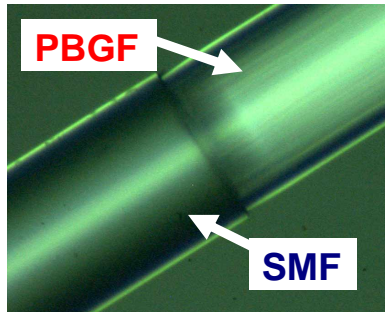

Fig. 3. A micrograph showing the splice between the SMF and 10.9 μm PBGF. Picture courtesy of the GaN Group in the Kansas State University Physics Department.

3. PBGF-SMF splice for a gas-filled PBGF cell

3.1 Absorption spectroscopy

One important application of PBGF-SMF splices is in the creation of gas-filled PBGF cells. Saturated absorption spectroscopy on such cells is a promising technology for portable optical frequency references, but sensitive to the splice quality. This sensitivity arises because light reflected from both splices can form a standing wave as in a Fabry-Perot cavity, and thus the fiber cell transmission depends periodically on optical frequency. This frequency-dependent "background" creates a shift in the apparent line center of the absorption feature of the reference gas, such as acetylene, and thus degrades the performance of the frequency reference.

The splices will be useful in a PBGF cell, as demonstrated using saturation spectroscopy on acetylene inside PBGF that is spliced to SMF fiber. Several different fibers and splices are then compared. The experimental set-up is shown in Fig. 4, and is similar to that of Ref. [4]. Here, a PBGF spliced to SMF is evacuated by pumping with a mechanical roughing pump on the PBGF's open end in a vacuum chamber. The fiber is evacuated to ~15 mtorr over 12 hours. Then the vacuum chamber and PBGF are filled with acetylene gas to a pressure of 0.9 torr. Absorption spectroscopy on the gas in the PBGF reveals a strong absorption feature. Light from a ~1531 nm tunable diode laser is amplified by an erbium-doped fiber amplifier and split to produce a probe (~1 mW) and pump (~30 mW). The probe beam passes through a double-passed acousto-optic modulator, an isolator, and a polarization controller, and then counter-propagates the pump beam through the PBGF. The transmitted probe beam power is detected by a photodetector as the diode laser frequency scans across the absorption feature. The laser is swept eight times across the signal, and the eight traces are averaged on an oscilloscope.
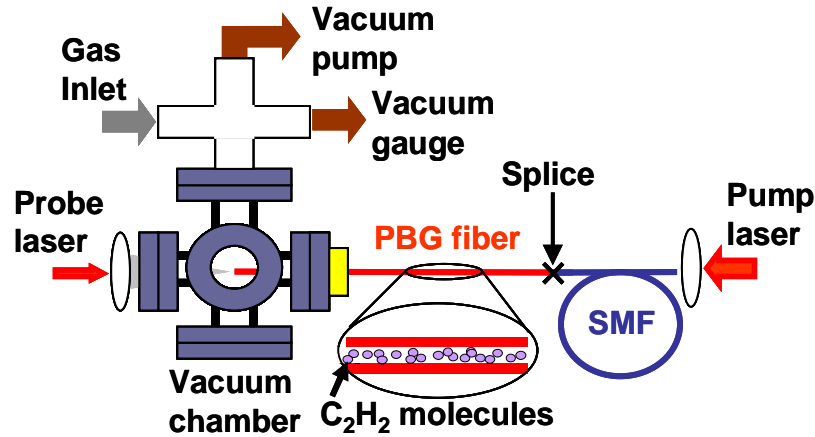
Fig. 4. Chamber used to evacuate and fill the PBGF with acetylene gas for saturated absorption spectroscopy.

Saturated absorption spectra are shown in Fig. 5; here the spectra between different 10.9 µm and 20 µm fibers are compared. Figure 5(a) compares three 10.9 µm PBGFs: Fiber 1 is 0.78 m long spliced to SMF with an arc splicer; Fiber 2 is 2.0 m long spliced to SMF with a commercial filament fusion splicer (spliced and purchased from Crystal Fibre) [12]; and Fiber 3 is 0.9 m long unspliced. Figure 5(b) compares two 20 µm PBGFs: Fiber 4 is 0.4 m long spliced to SMF with an arc splicer as described above, and Fiber 5 is 0.78 m long unspliced. Two vacuum chambers were used to perform the saturation spectroscopy on the unspliced PBGFs [4]. The 10.9 µm fibers exhibit some dependence of transmission with frequency, with similar interference fringe contrast ratios of ~5%-10%. In contrast, the 20 µm fiber splices exhibit much smaller interference fringe contrast ratios of less than 0.5%. Thus these fringes are not thought to arise from the splice, but rather to be intrinsic to the fiber, due for example to mode beating associated with the excitation of surface modes. In both cases the splice does not significantly impact the quality of the saturated absorption feature. Of course, a fiber cell requires two splices, one of which can be made by the above method. Further investigations will be required to characterize and minimize the impact of reflections from a second splice on the signal quality of the cell.
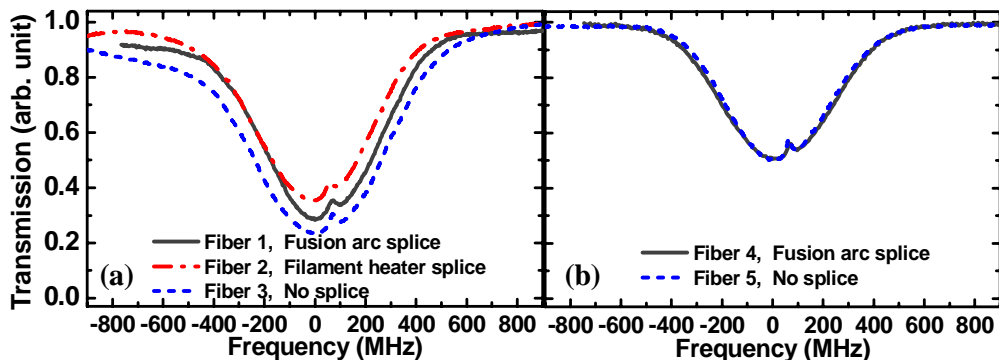

Fig. 5. Saturated absorption spectra in (a) 10.9 µm and (b) 20 µm diameter PBGFs. Fiber 1 is 0.78 m long, spliced to SMF using a conventional arc splicer using the technique described in this paper. The P(11) spectrum was taken at 29 mW and 0.9 torr. Fiber 2 is 2.0 m long, spliced to SMF by Crystal Fibre A/S using a filament heating splicer, and its spectrum is taken of the weaker P(12) transition at 17 mW and 0.8 torr. Fiber 3 is the unspliced 10.9 µm fiber of 0.9 m long, the P(11) spectrum was taken at 30 mW of pump power at 0.6 torr. Fiber 4 is 0.4 m long, spliced with an arc splicer to SMF, the P(11) spectrum was taken at 34 mW and 0.9 torr. Fiber 5 is unspliced fiber 0.78 m long, and the P(11) spectrum was taken at 29 mW of pump power at 0.7 torr.

4. Summary

We have demonstrated a repeatable, low-loss fusion splice between PBGF and SMF using a commercial arc fusion splicer whose loss compares well to splices made with a filament fusion splicer. The minimum observed splice loss is consistent with expected losses due to mode field mismatch, while the asymmetry is attributed to the multimode nature of the PBGF. Furthermore, the splice did not degrade the quality of saturated absorption spectra when used at one end of a gas-filled fiber cell. Future work will involve sealing the PBGF with a second low loss splice in an acetylene atmosphere while filling the PBGF, using a CO_2 laser.

Acknowledgments